TÜBİTAK

Turkish Journal of Chemistry

http://journals.tubitak.gov.tr/chem/

Research Article

Turk J Chem
(2019) 43: 125 – 136
© TÜBİTAK
doi:10.3906/kim-1807-59

Novel "turn off-on" sensors for detection of DNA-acrylamide interaction using ZnS quantum dots as a phosphorescent probe

Hayriye Eda ŞATANA KARA*
Department of Analytical Chemistry, Faculty of Pharmacy, Gazi University, Ankara, Turkey

Received: 13.07.2018 • **Accepted/Published Online:** 19.10.2018 • **Final Version:** 05.02.2019

Abstract: A novel "turn off-on" sensor for detection of interaction between DNA and acrylamide (ACR) was developed. In this method, L-cysteine capped Mn-doped ZnS quantum dots (QDs) were used as room temperature phosphorescent probes. In the "turn-off" mode, ACR was absorbed onto the surface of QDs via electrostatic interaction, which caused a quenching effect of room-temperature phosphorescence signal by photoinduced electron-transfer mechanism. ACR was removed from the QDs' surface with the addition of DNA. Thus, the phosphorescence emission of QDs was recovered and the system was turned to the "turn-on" mode. The quenching mechanism of QDs by ACR was collisional (dynamic) and the quenching constant, binding constant, and binding site number were calculated as 3.2×10^4 M^{-1}, 2.04×10^4 M^{-1}, and 1.2, respectively. An absorption spectrometric method was also used to evaluate ACR-DNA interaction and the binding constant (K) was found as 2.4×10^5 M^{-1}. The developed biosensor is simple, is free of interferences coming from autofluorescence and scattering light, and does not need any derivatization step or sample pretreatment.

Key words: Acrylamide, DNA interaction, quantum dots, phosphorescence, photoinduced electron transfer

1. Introduction

Acrylamide (ACR) is a chemical compound (C_3H_5NO) (Figure 1) that forms at a high temperature during the cooking process, generally in starch-rich food samples. The major formation pathway of ACR is the Maillard reaction, which is based on the reaction between an amino acid and the carbonyl group of reducing sugar. ACR is also used as a chemical reagent in molecular biology laboratories, polymer synthesis, wastewater treatment, cosmetics, food packing, and pesticide formulations.[1,2] People may be exposed to ACR by food intake and skin absorption. After intake into the human body, the ACR is metabolically converted to the genotoxic metabolite glycidamide by cytochrome P450 enzyme in the liver. The major ACR sources are foods such as French fries, potato chips, roasted coffee, bread, and cereals. These may include ACR at µ g/kg levels.[3] The ACR levels in these samples depend on the ingredients, cooking process, cooking time, and temperature. ACR has been considered a potential carcinogen by International Agency for Research on Cancer, the European Union, and the World Health Organization.[4] For this reason, DNA-ACR interaction studies are important to understand the effect of the compound in the human body.

DNA is the main target molecule for drugs, carcinogens, and environmentally toxic substances. Because it is genetic material, the interaction of DNA and carcinogenic molecules causes chromosome abbreviations and finally cell death. Consequently, the evaluation of DNA-small molecule interactions is important for the

*Correspondence: eda@gazi.edu.tr

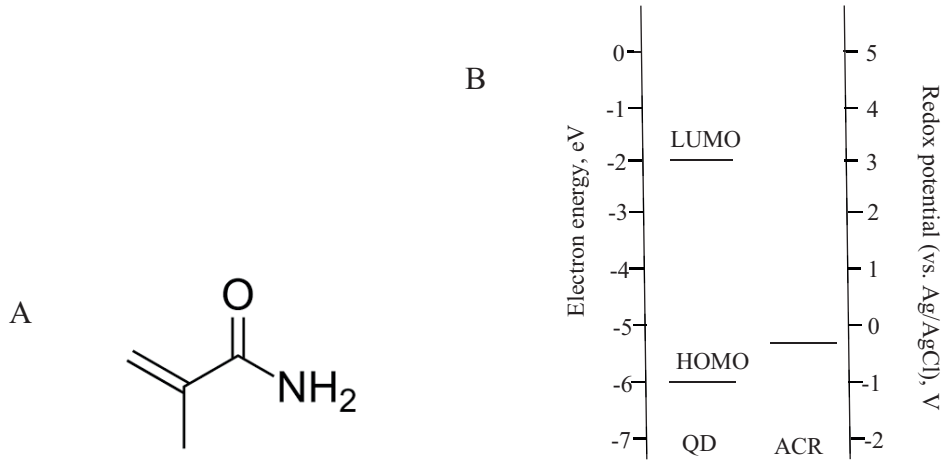

Figure 1. (A) Chemical structure of ACR and (B) energy diagram of QDs and redox potential of ACR.[28,29]

understanding of the effect mechanism of molecules. For this purpose, different techniques were used and developed for the evaluation of the interaction of DNA-small molecules. These methods are generally based on spectroscopic (circular dichroism, UV-Vis, fluorescence, phosphorescence, NMR, etc.)[5–8] and electrochemical techniques.[9,10]

Phosphorescence is a type of photoluminescence associated with "forbidden" energy state transitions in quantum mechanics. This transition occurs from the excited triplet state (T_1) to the singlet ground state (S_0). These slow transitions cause emission at a longer wavelength with longer lifetime, which allows avoiding spectral interferences.[11]

Quantum dots (QDs) are semiconductor luminophore nanoparticles that possess unique luminescence properties. They have broad absorption and narrow emission bands, which are tunable with their particle sizes. However, their luminescent properties are also changed with doping. For example, doping of Mn^{2+} into ZnS QDs causes energy transfer from the bandgap transition of ZnS to Mn^{2+}. This event leads to formation of new emission centered at around 590 nm. Large Stokes shift and long-lived emission act as keys for avoiding self-absorption and spectral interferences. In addition to this, QDs have high photoluminescence quantum yield and photo/chemical stability.[12–14] In pharmaceutical and biomedical analysis, QDs are widely used as a luminescent probes because of their advantages over organic dyes.[15–18]

The developed methods using QDs are generally based on the quenching of fluorescence/phosphorescence intensity of nanoparticles. Although the application of this "turn-off" system is very easy, low signal to noise ratio and sensitivity to the interference of other substances cause limited application. In order to overcome these problems, the "turn off-on" system has been developed. In this technique, in the first step, the intensity of QDs is decreased due to interaction with the quencher, and in the second step, the emission intensity is recovered by desorption of quencher from the QDs' surface because of the competitive reaction of quencher and analyte. This system has been successfully used for the detection of pharmaceuticals, DNA, enzymes, ions, and viruses[7,19–21] due to its improved specificity.

In this study, a novel room-temperature phosphorescence (RTP) "turn off-on" system is reported in order to evaluate the mechanism of ACR-DNA interactions. In the literature, a few studies, which used electrochemical methods, have been reported for the investigation of ACR and DNA interaction. Working mechanisms of these

developed electrochemical biosensors are based on interaction of ACR and guanine bases of double-stranded DNA (ds-DNA) or single-stranded DNA (ss-DNA) at the N-7 position.[22,23] Although DNA and ACR interaction was studied by these methods, this is the first report on the application of RTP using QDs for the identification of DNA-ACR interaction. In the developed method, L-cysteine capped Mn-doped ZnS QDs and ACR form nanohybrids, which cause quenching of RTP emission intensity of QDs, and, in this way, the "turning off" part is realized. The "turning on" part occurs by means of groove binding with DNA. Formation of the ACR-DNA complex leads to desorption of ACR from the QDs' surface so that the RTP intensity of QDs is recovered. Based on this method, a new biosensor was established to identify the DNA-ACR interaction. The developed method has advantages such as sensitivity, selectivity, simplicity, cheapness, and short analysis time compared to other methods. In addition, UV-Vis spectrophotometry was also used for better understanding the interaction mechanism.

2. Results and discussion

2.1. Characterization of the Mn-doped ZnS QDs

L-cysteine capped Mn-doped ZnS QDs were synthesized in aqueous solution using zinc sulfate, manganese chloride, and sodium sulfide. L-cysteine was selected as a capping agent and gave a water-soluble character to the QDs. This specification not only protects the QDs from aggregation but also provides for specific binding of QDs to a target molecule, which causes formation of QD-drug nanohybrids. At the studied pH (7.4), QDs' surface and the ACR have negative and positive charges, respectively. Therefore, electrostatic interaction between ACR and QDs occurs.

In previous studies, morphologies of QDs were identified[24] as spherical with a diameter of about 3.5 nm. To verify this result, Eq. (1) was used to calculate the diameter of Mn-doped ZnS QDs:[25]

$$\Delta E(r) = E_g(r) + h^2 /8r^2(1/m_e^* + 1/m_h^*), \quad (1)$$

where ΔE is the emission energy, E_g is band gap energy, r is the radius, h is the Planck constant, m_e^* is the effective mass of the excited electron, and m_h^* is the effective mass of the excited hole. From this equation, the diameter of the prepared Mn-doped ZnS QDs was calculated at about 3.5 nm.

2.2. Spectral properties of the Mn-doped ZnS QDs

UV-Vis spectra of the prepared QDs showed that QDs have a broad band between 250 nm and 320 nm with a maximum at 290 nm (Figure 2).

In phosphorescence spectra, the maximum excitation peak of QDs occurred at 290 nm and the narrow and symmetrical main emission peak was at 590 nm. The observed orange phosphorescence emission was attributed to the energy transfer from the band gap of ZnS to the dopant Mn^{2+} and triplet to ground state transition of the Mn^{2+} incorporated into the lattice of ZnS.[26] In addition, in the synthesis step, aging at 50 °C for 2 h is more important to form QDs. There is no peak observed unless heat treatment is applied (Figure 2).

For the determination of photoluminescence quantum yield of prepared QDs, quinine (Φ = 0.546 in 0.5 M H_2SO_4) was used as a reference standard and it was calculated as 20.4%.[27]

The phosphorescence signal of prepared water-soluble L-cysteine capped Mn-doped ZnS QDs was very stable when they were kept in darkness at 4 °C for at least 6 months without remarkable precipitation.

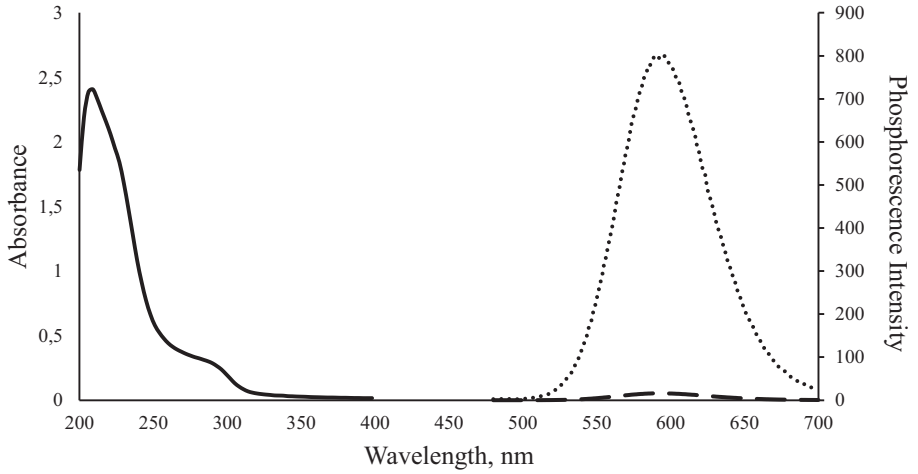

Figure 2. The absorption (¦), heated (….), and unheated (—) phosphorescence spectra of Mn-doped ZnS QDs.

2.3. Factors affecting phosphoresce intensity of QDs

The effects of several factors such as pH and reaction time on the RTP intensity of L-cysteine Mn-doped ZnS QDs and its nanohybrids were analyzed.

The studies showed that pH is highly effective on phosphorescence intensity of QDs. In the acidic area (pH 5–7), the RTP intensity of L-cysteine capped Mn-doped ZnS QDs was low. The RTP intensity was rapidly enhanced with the increment of pH between 7.4 and 8.0, and it was weakened again in the basic area (pH <8). Similar behavior was observed for the quenched phosphorescence signal, which also changed with pH. The obtained results explained that the developed sensor was stable within pH 7.0–8.0 and thus pH 7.4 was selected as the optimal value (Figure 3A).

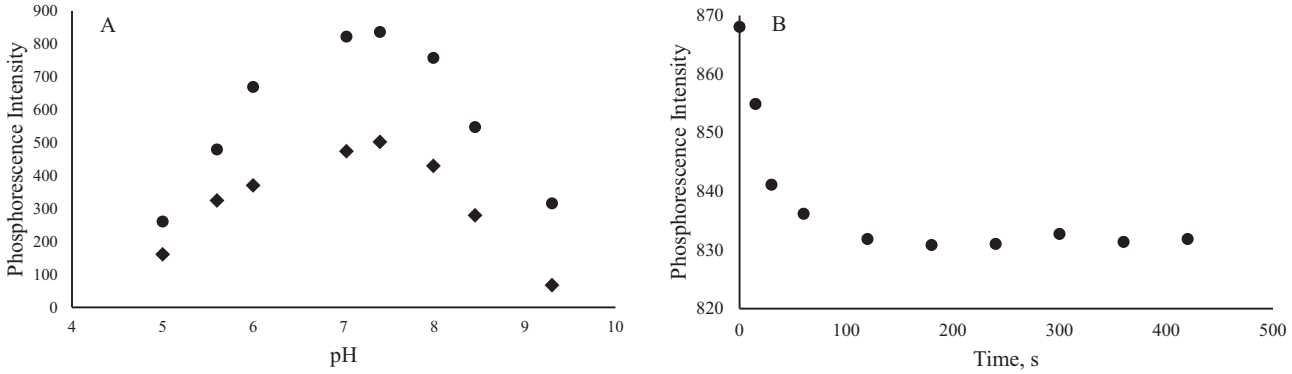

Figure 3. (A) pH effect on the RTP intensity of QDs (●) and the quenched intensity of QDs (⧫); (B) the effect of reaction time on the quenched RTP intensity of QDs (0 s is RTP signal of QDs only).

The effect of reaction time was also identified. As shown in Figure 3B, when ACR was added to the QD solution, the RTP intensity was quenched rapidly. The equilibrium in the interaction requires about 2 min after this time signal is stable. For this reason, 2 min was selected as the analysis time.

2.4. Interference studies of Mn-doped ZnS QD "turn off-on" probes

The interference effects of some common ions and biomolecules in biological fluids on DNA-ACR interaction were investigated. For this purpose, glucose; some selected ions, such as Ca^{2+}, Mg^{2+}, K^{+}, and Na^{+}; amino acids and proteins, such as dopamine, creatinine, cholesterol, L-cysteine, and L-cystine; and acrylic acid and methacrylic acid, which are ACR-like molecules, were added to QDs, QD-ACR, and QD-ACR nanohybrids including DNA solutions. There were no interfering effects at 100-fold glucose, 500-fold cations, 100-fold amino acids-proteins, and 100-fold ACR-like molecules, which means that the developed "turn off-on" RTP probe was highly selective (data not shown). Obtained results showed that the proposed probe may be used for the evaluation of ACR-DNA interaction in biological samples without potential interferences.

2.5. Evaluation of DNA-ACR by using RTP "turn off-on" probes

The interaction of DNA-ACR was evaluated by using the L-cysteine capped Mn-doped QDs as a "turn off-on" RTP probe. This method is based on measurement of the changing of RTP intensity of QDs with addition of ACR and DNA. The natural RTP emission of QDs was quenched by ACR, and after adding DNA, ACR was released from the surface due to formation of a new ACR-DNA complex and recovery of the RTP signal occurred (Scheme).

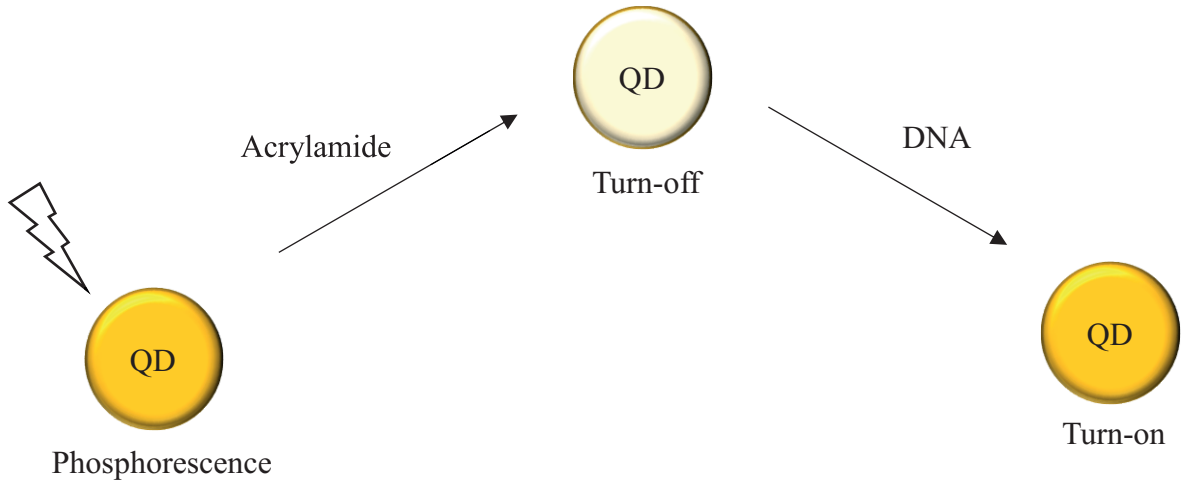

Scheme. A schematic illustration of "turn off-on" strategy of Mn-doped ZnS QDs/ACR nanohybrids for DNA detection.

At the studied pH (7.4), prepared QDs have a negative charge because of the L-cysteine while ACR has a positive charge due to the amine group. Therefore, ACR-QD nanohybrids were formed by electrostatic interaction and this caused the quenching of the RTP intensity of QDs. This quenching mechanism was based on photoinduced electron-transfer (PIET) reaction. The reduction potential of ACR was found at about –0.25 V[28] and the HOMO and LUMO energy levels of QDs vs. vacuum were calculated as –6.0 and –2.0 eV.[29] These results explained that the ACR and QDs were electron acceptors and donors, respectively (Figure 1).

The phosphorescence quenching process takes place in two ways: static and collisional or dynamic. In the first system, the quencher and phosphorescent molecules interact at the ground state and form a new nonphosphorescent complex. For the second quenching process, the molecules are in contact in the excited state and finally nonradiative relaxation occurs. These two quenching mechanisms can be differentiated from each

other by different behaviors against temperature and viscosity. At high temperature, static quenching decreases because of breaking of weak bonds between the phosphorescent molecules and the quencher, while dynamic quenching tends to increase due to fast diffusion. Besides that, in static quenching, the lifetime of RTP does not change. However, for dynamic quenching, the decreasing of intensity and lifetime is observed due to the interaction of molecules in the excited state. Generally, although only one quenching process is observed, in some cases, both processes can occur simultaneously. In this condition, Stern–Volmer plots change from linear to an upward curvature.[30]

Lineweaver–Burk (Eq. (2)) and Stern–Volmer (Eq. (3)) equations can be used to identify the type of quenching;

$$1/(P_0 - P) = 1/P_0 + K_{LB}/(P_0[Q]), \tag{2}$$

$$P_0/P = 1 + K_{SV}[Q], \tag{3}$$

where P_0 and P are the phosphorescent intensity of the phosphorescent molecule, here QDs, in the absence and presence of the quencher, respectively. [Q] is the concentration of the quencher. K_{LB} and K_{SV} are the static and dynamic quenching constants, respectively. K_{SV} is the Stern–Volmer quenching constant, determined by linear regression of a plot of P_0/P against [Q]. However, the linear relationship between $1/(P_0 - P)$ and [Q] helps to determine K_{LB}.

In the present study, the phosphorescence intensity of L-cysteine capped Mn-doped ZnS QDs was quenched by the addition of ACR (Figure 4). The relationship between P_0/P and the concentration of ACR followed Stern–Volmer equation and a linear plot ($r^2 = 0.993$) was obtained, while the plot of the Lineweaver–Burk equation has a curve character instead of linearity (Figure 5). According to the obtained results, ACR and QDs interacted in the excited state, which leads to dynamic quenching, and K_{SV} was found to be 3.2×10^4 M^{-1}, which means that ACR-QD interaction was moderate.

The number of binding sites (n) and binding constant of ACR with QDs were calculated by using

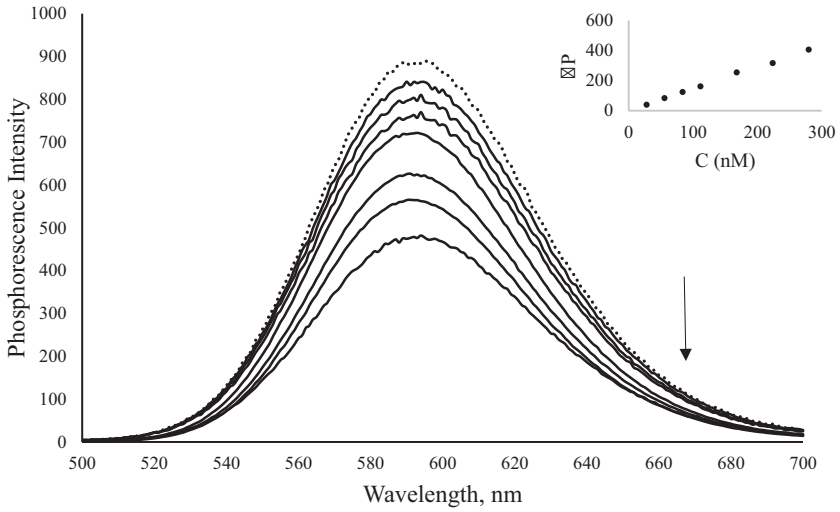

Figure 4. ACR concentration-dependent RTP intensity of QDs (dotted line is QDs alone). The concentrations of ACR were 28–56–84–112–168–224–280 nM (top to bottom). The inset shows the change of the RTP intensity with the increase of the ACR concentration.

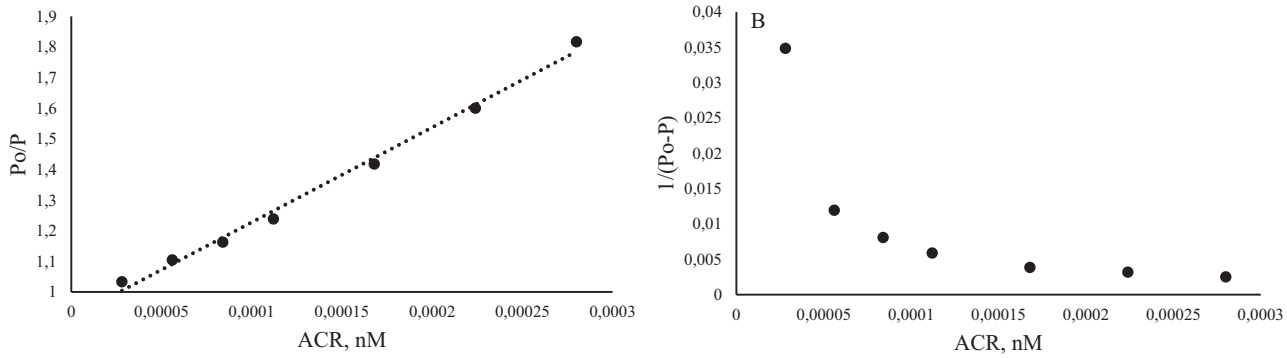

Figure 5. (A) Stern–Volmer and (B) Lineweaver–Burk plots for the RTP quenching effect of ACR on QDs.

Eq. (4):

$$\log(F_0 - F)/F = \log K + n \log[Q], \tag{4}$$

where K is the binding constant and n is the number of the binding site, which can be determined by the ordinate and slope of the logarithmic regression curve of log (F_0 – F)/F versus log[Q], respectively. n and K were found as 1.24 and 2.04 $\times$ 10^4 M^{-1}, respectively. The calculated binding constant was less than the binding constant of ACR-DNA, which means that ACR-QD interaction was weaker than the ACR-DNA interaction force. Therefore, the developed method was suitable for evaluation of ACR-DNA interaction.

Figure 6 shows the detection of DNA-ACR interaction by using QD-ACR nanohybrids as phosphorescent probes. In the beginning, the RTP intensity of QDs was quenched by adding ACR. After addition of DNA, the gradually and regularly enhanced intensity of QD-ACR nanohybrids was observed.

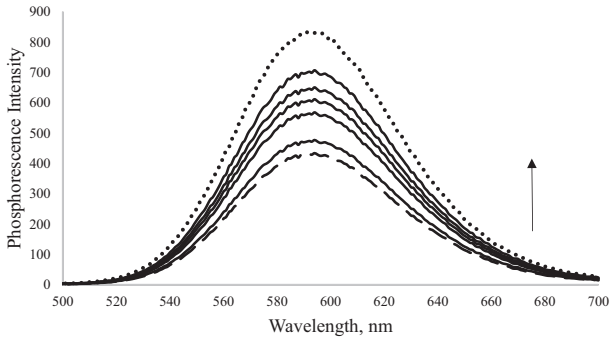

Figure 6. Phosphorescence spectra of Mn-doped ZnS QD-ACR nanohybrids after adding 0.3, 0.6, 0.9, 1.8, and 2.4 µ M ds-DNA (bottom to top; dotted line and dashed line are QD and QD-ACR nanohybrid spectra, respectively).

At pH 7.4, the L-cysteine capped Mn-doped ZnS QDs were negatively charged; however, ACR became a good electron acceptor because the surface of ACR is positive. Therefore, QD-ACR nanohybrids were formed by electrostatic interaction. The PIET mechanism between the QDs and ACR caused the quenching of phosphorescence intensity and "turn-off" mode was realized.

In order to realize the "turn-on" mode, the RTP intensity of QD-ACR nanohybrids was recovered with the increment of DNA content (Figure 6). This result showed that ACR was released from the QDs' surface by adding DNA, and it formed a new and more rigid complex with DNA, which caused the recovery of the RTP intensity. This can be explained as follows: as reported in the literature, ACR is not only a good hydrogen bond acceptor but also a good hydrogen bond donor to highly electronegative atoms such as O and N.[22] Thus, ACR

can form stable hydrogen bonds with purine and pyrimidine bases of DNA, which cause formation of a stable DNA-ACR adduct. In addition, the strength of the hydrogen bond between ACR and guanine is strong enough to break the bond between guanine and cytosine, which allows formation of a new ACR-guanine complex.[31]

At neutral and basic pH, the interaction between nucleophilic groups of DNA bases and the ACR may be a hydrophobic interaction rather than a nucleophilic interaction due to the conversion of DNA to anionic form. In addition, in the absence of ACR, the RTP intensity of QDs was quenched less severely and the ratio of P and P_0 was around 1. This is because at the studied pH (7.4), QDs and DNA were both negatively charged and their interaction was very weak.

In order to determine of repeatability of the developed sensor, all experiments were repeated five times and the RSD% value was found to be less than 2%.

2.6. Phosphorescence lifetime

Phosphorescence lifetimes of QDs, QD-ACR nanohybrids, and the QD-ACR/DNA system were evaluated by using their phosphorescence emission decay curves. As shown from Figure 7, the lifetime of QDs was decreased from 8.89 ms to 7.05 ms due to changing of the electron transfer process and quenching effect. However, with the addition of DNA, a new complex formed between ACR and DNA, and, as a result, ACR was released from the QDs' surface, which increased the phosphorescence lifetime to 7.36 ms. As mentioned before, the changing of lifetime of QDs with the addition of ACR showed that the quenching mechanism was dynamic.

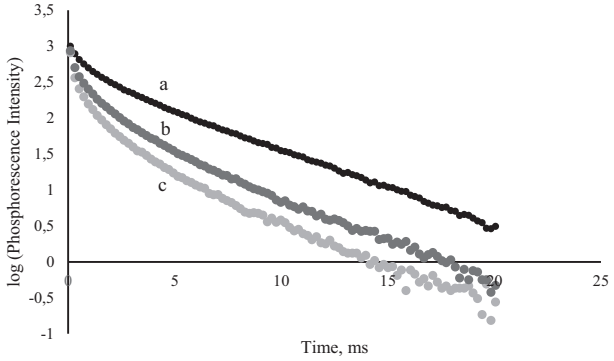

Figure 7. Phosphorescence lifetime of QDs (line a), QD-ACR nanohybrids (line c), and QDs-ACR with DNA (line b).

2.7. Absorbance experiments

Absorbance spectroscopy is a commonly used method for the investigation of binding characteristics and interaction between DNA and small molecules. Well-known interactions are electrostatic, which occurs between the phosphate group of DNA and the charged group of molecule; intercalation, where molecules and especially those containing aromatic groups settle in the DNA helix; and interactions in which the molecule engages the minor/major groove of DNA, which is called groove binding. In all three cases, the absorption spectra of DNA and/or the molecule change.[32] The interaction of a small molecule and DNA forms a new complex molecule, whose absorbance spectra are different from each other. Generally, these differences can be decreasing (hypochromicity) or increasing (hyperchromicity) of absorbance value and/or red (bathochromic) or blue (hypsochromic) shift. Ordinarily, red shifts and the decreasing of absorbance intensity are observed at stronger binding modes, such as intercalation due to π-π stacking from the aromatic planar structure and the base pairs

of DNA. In weak interactions such as electrostatic or groove binding, a decrease of the absorbance intensity is observed, similarly to the intercalative mode, but shifting does not appear. Consequently, the interaction can be evaluated by using spectra before and after the interaction reaction.[7]

In order to investigate the interaction mechanism of ACR and DNA, the spectrophotometric titration method was used. The UV-Vis spectrum of DNA shows a broad band spectrum 200 and 350 nm and has maximum absorption at 260 nm due to chromophore groups at purine and pyrimidine bases. However, ACR has no absorbance in the studied media. Therefore, only DNA spectra were followed before and after interaction reaction. In the studied media (pH 4.5), the NH_2 group of ACR is positively charged and the electrostatic interaction occurred between the ACR and the negative phosphate groups of DNA. In addition, regarding the isoelectric point of DNA, hydrogen bonds were also formed between ACR and DNA bases.

The $–NH_2$ group of ACR has affinity for the guanine base of the DNA structure. Thus, hydrogen bonds between N-H-N and N-H-O may be formed when ACR interacts with DNA. Experimental results show that acidic media are more favorable for ACR-DNA binding. Depending on the isoelectric point of DNA, at pH 4–4.5, it is more likely that H-bonds are formed between $–NH_2$ of ACR and DNA's bases. Moreover, $–NH_2$ groups of ACR are positively charged in acidic media, which allows for the electrostatic attraction between the negative phosphate group of DNA and $–NH_2^+$ of ACR.[33]

Figure 8 shows the absorption spectra of DNA and the ACR-DNA complex. DNA has a main peak at 260 nm. A significant decrease in absorption of DNA and a slight red shift (4 nm) were observed with the addition of ACR. This hypochromic effect and the shifting were attributed to the interaction of ACR and DNA by groove binding with electrostatic forces (Figure 8).

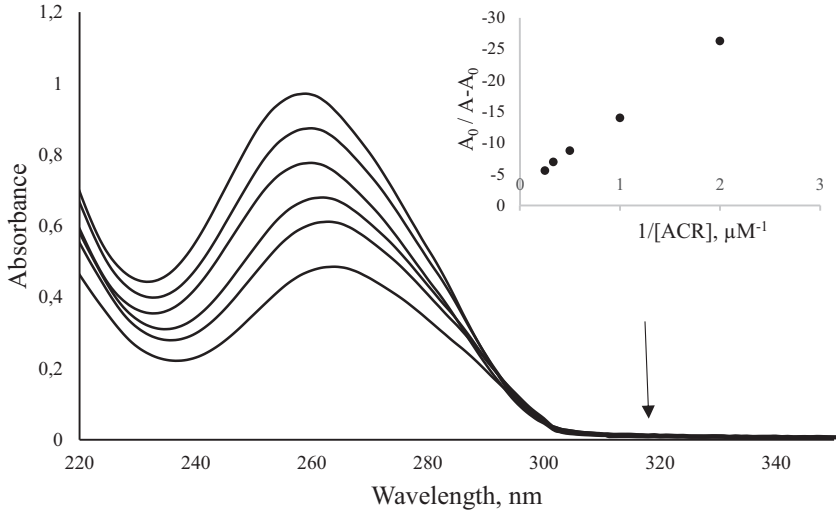

Figure 8. Absorption spectra of DNA in the presence of ACR at different concentrations. C_{DNA} = 9 µ M and C_{ACR} = 0.5, 1.0, 2.0, 3.0, and 4.0 µ M.

A spectrophotometric titration method was used for the determination of ACR-DNA interaction. According to the obtained spectra, the Benesi–Hildebrand equation (Eq. (5)) was used for the calculation of the binding constant (K):[34]

$$A_0/(A - A_0) = \varepsilon/(\varepsilon_0 - \varepsilon) + \varepsilon/(\varepsilon_0 - \varepsilon) \times 1/K[DNA], \quad (5)$$

where A_0 and A are the absorbance values of DNA in the absence and presence of ACR, respectively. ε_0 and

ε are the absorption coefficients of DNA and its complex with ACR, respectively. The plot of $A_0/(A - A_0)$ vs. 1/[ACR] was drawn using the data from the spectrophotometric titrations and a linear fitting of the data yielded the binding constant (K), which was 2.4×10^5 M^{-1} for DNA-ACR (Figure 8, inset). This value indicates a strong interaction between ACR and DNA.

2.8. Conclusions

In this paper, L-cysteine capped Mn-doped ZnS QDs were synthesized and characterized. Prepared QDs were used for the forming of QD/ACR nanohybrids, which were used for investigation of the interaction between ACR and DNA as novel RTP sensors.

The adsorption of ACR onto the QDs' surface via PIET mechanism caused quenching of RTP intensity of the QDs. The probable quenching mechanism was dynamic. DNA addition produced a new complex between ACR and DNA; thus, restoration of the RTP signal took place by desorption of ACR from the QDs' surface. Using this method, the detection of DNA could be realized in the biological samples via the relationship of phosphorescence intensity and quantity.

The proposed RTP method is free of interferences coming from ions, amino acids, autofluorescence, and scattering light. Besides, compared to the other conventional RTP methods, the QD-based RTP technique does not require surfactants, heavy ion, deoxidants, or any other chemical modifiers.

For better understanding of the interaction, UV-Vis spectrophotometry was also used. The absorption spectra showed that absorbance values of DNA decreased with the addition of ACR and a slight red shift was observed. These results showed that ACR and DNA interacted by groove binding mode via electrostatic forces.

The obtained results from the interaction mechanism of ACR and DNA would help to understand the binding of other potential cancer molecules to DNA.

3. Experimental

3.1. Materials and chemicals

Calf thymus double-stranded DNA was obtained from Sigma-Aldrich (St. Louis, MO, USA) and ACR, $ZnSO_4$, $MnCl_2$, Na_2S, and L-cysteine were obtained from Merck (Darmstadt, Germany). Deionized water (18.2 MΩcm, Simplicity, Milli-Q Millipore water purification system) was used for the preparation of aqueous solutions. Sodium hydroxide, acetic acid, and phosphoric acid were analytical grade reagents and they were prepared in deionized water.

3.2. Apparatus

Phosphorescence measurements were done with a Cary Eclipse fluorescence spectrophotometer (Varian, USA) equipped with a quartz cuvette (10 × 10 mm) and a Xenon flash lamp was used as the light source. For phosphorescence experiments, excitation and emission wavelengths were 290 and 590 nm, respectively.

UV-Vis spectra were recorded using a Specord 50 Plus (Analytik Jena, Germany) with a 10 × 10 mm path length quartz cell.

The pH measurements were performed using a combined pH electrode with an Orion model 720 A pH meter. All experiments were performed at room temperature.

3.3. Synthesis of the Mn-doped ZnS QDs

L-cysteine Mn-doped ZnS QDs were synthesized in aqueous solutions according to a published method.[35] First, 5 mL of 0.1 M $ZnSO_4$, 1.5 mL of 0.01 M $MnCl_2$, and 50 mL of 0.02 M L-cysteine were added to a three-necked flask. Using 1 M NaOH, the pH of the solution was adjusted to 11.0. At room temperature, argon gases were passed through the mixture for 30 min for removing the air. After ventilation, 5 mL of 0.1 M Na_2S was injected into the mixture. After stirring for 20 min, the solution was aged at 50 °C under open air for 2 h to form L-cysteine capped Mn-doped ZnS QDs.

3.4. Assay conditions

Phosphate buffer (20 mM, pH 7.4) for phosphorimetric measurements and acetate buffer (20 mM, pH 4.5) for spectrophotometric measurements were prepared with deionized water and pH was adjusted using sodium hydroxide (5 M).

In order to prepare the stock ACR solution, 5 mg of ACR was weighed accurately and dissolved in 10 mL of deionized water. Working solutions of ACR were prepared by dilution of the appropriate quantity in buffer solution.

The DNA solution was prepared by dissolving 5.0 mg in 10.0 mL of deionized water. The prepared solution was kept in a refrigerator for one night to dissolve the fibers completely. Absolute concentration was determined spectrophotometrically by using the Beer–Lambert law (ε_{260} = 6600 L mol^{-1} cm^{-1}) and was found at about 1.51 × 10^{-4} M. The absorbance ratio A_{260}/A_{280} gives the purity of the DNA solution,[7] which should be between 1.8 and 1.9. This value indicated that DNA samples did not include any interferents coming from tissue or cells proteins such as tryptophan or tyrosine. The ratio of absorbance values was found as 1.83, which demonstrated that the protein concentration was negligible and the DNA was pure.

3.5. DNA-ACR interaction studies

For studying the ACR effect on the RTP intensity of QDs, a manual spectrophotometric titration method was used. The assay solutions containing L cysteine-capped Mn-doped ZnS QDs (100 µ L) were prepared in 20 mM phosphate buffer, pH 7.4. The aliquot from the stock ACR solution was added as 2.0 µ L to avoid a change in the volume. Measurements were done 2 min later after the addition to complete the reaction. The calibration graph was constructed using a plot of P_0/P against [Q]. In order to evaluate the DNA-ACR interaction, DNA solution was added to a solution including QD-ACR nanohybrids.

To detect UV-Vis absorption spectra of DNA and ACR, solutions were prepared, each in 10 mL of acetate buffer (20 mM, pH 4.5). For interaction studies, 9 µ M DNA in 2.5 mL of buffer solution was titrated manually by successive additions of ACR solutions. Measurements were performed 2 min after mixing. In order to avoid a change in the volume, each addition was 2.0 µ L. The reference solution was an acetate buffer.

References

1. Mottram, D. S.; Wedzicha, B. L.; Dodson, A. T. *Nature* **2002**, *419*, 448-449.
2. Stadler, R. H.; Blank, I.; Varga, N.; Robert, F.; Hau, J.; Guy, P. A.; Robert, M. C.; Riediker, S. *Nature* **2002**, *419*, 449-450.
3. Keramat, J.; LeBail, A.; Prost, C.; Soltanizadeh, N. *Food Bioprocess Technol.* **2011**, *4*, 340-363.
4. Dybing, E.; Farmer, P. B.; Andersen, M.; Fennell, T. R.; Lalljle, S. P. D.; Muller, D. J. G.; Olin, S.; Peterson, B. J.; Schlatter, J.; Scholz, G. et al. *Food Chem. Toxicol.* **2005**, *43*, 365-410.

5. Alam, M. F.; Varshney, S.; Khan, M. A.; Laskar, A. A.; Younus, H. *Int. J. Biol. Macromol.* **2018**, *113*, 300-308.
6. Huang, J. H.; Wang, X. M.; Fei, D.; Ding, L. S. *Appl. Spectrosc.* **2010**, *64*, 1126-1130.
7. Ozluer, C.; Kara, H. E. S. *J. Photoch. Photobio. B* **2014**, *138*, 36-42.
8. Gao, X. L.; Patel, D. J. *Q. Rev. Biophys.* **1989**, *22*, 93-138.
9. Kara, H. E. S. *Bioelectrochemistry* **2014**, *99*, 17-23.
10. Yola, M. L.; Ozaltin, N. *J. Electroanal. Chem.* **2011**, *653*, 56-60.
11. Kuijt, J.; Ariese, F.; Brinkman, U. A. T.; Gooijer, C. *Anal. Chim. Acta* **2003**, *488*, 135-171.
12. Frasco, M. F.; Chaniotakis, N. *Sensor* **2009**, *9*, 7266-7286.
13. Resch-Genger, U.; Grabolle, M.; Cavaliere-Jaricot, S.; Nitschke, R.; Nann, T. *Nat. Methods* **2008**, *5*, 763-775.
14. Roya, Z.; Mansour, B.; Afshin, M.; Gamal, H. H. *Clin. Biochem.* **2011**, *44*, S223.
15. Gholami, S.; Kompany-Zareh, M. *Anal. Bioanal. Chem.* **2013,** *405*, 6271-6280.
16. Sinduja, B.; John, S. A. *Spectrochim. Acta A* **2018,** *193*, 486-491.
17. Muhammad, S.; Xu, G. H.; Wei, F. D.; Ma, Y. J.; Ma, Y. S.; Song, Y. Y.; Shi, M. L.; Xu, X. M.; Cen, Y.; Hu, Q. *Nanomaterials* **2017**, *7*, E358.
18. 18. .Bajwa, N.; Mehra, N. K.; Jain, K.; Jain, N. K. *Artif. Cell. Nanomed. B* **2016**, *44*, 758-768.
19. 19. Liu, X. T.; Na, W. D.; Qu, Z. Y.; Su, X. G. *RSC Adv.* **2016**, *6*, 85795-85801.
20. 20. Meng, A.; Xu, Q. H.; Zhao, K.; Li, Z. J.; Liang, J.; Li, Q. D. *Sensor. Actuat. B* **2018**, *255*, 657-665.
21. 21. Chen, L.; Zhang, X.; Zhang, C.; Zhou, G.; Zhang, W.; Xiang, D.; He, Z.; Wang, H. *Anal. Chem.* **2011**, *83*, 7316-7322.
22. 22. Huang, S.; Lu, S.; Huang, C.; Sheng, J.; Zhang, L.; Su, W.; Xiao, Q. *Sensor. Actuat. B* **2016**, *224*, 22-30.
23. 23. Li, D.; Xu, Y. M.; Zhang, L.; Tong, H. X. *Int. J. Electrochem. Sc.* **2014**, *9*, 7217-7227.
24. 24. He, Y.; Wang, H. F.; Yan, X. P. *Anal. Chem.* **2008**, *80*, 3832-3837.
25. 25. Şatana Kara, H. E.; Demirhan, B.; Er Demirhan, B. *Turk. J. Chem.* **2016**, *40*, 762-771.
26. 26. Chung, J. H.; Ah, C. S.; Jang, D. J. *J. Phys. Chem. B* **2001**, *105*, 4128-4132.
27. 27. Brouwer, A. M. *Pure Appl. Chem.* **2011**, *83*, 2213-2228.
28. 28. Vesela, H.; Sucman, E. *Czech J. Food Sci.* **2013**, *31*, 401-406.
29. 29. Zhao, T.; Hou, X. D.; Xie, Y. N.; Wu, L.; Wu, P. *Analyst* **2013**, *138*, 6589-6594.
30. 30. Lakowicz, J. R. *Principles of Fluorescence Spectroscopy*; Plenum Press: New York, NY, USA, 1999.
31. 31. Qiu, Y.; Qu, X.; Dong, J.; Ai, S.; Han, R. *J. Hazard. Mater.* **2011**, *190*, 480-485.
32. 32. Kennard, O. *Pure Appl. Chem.* **1993**, *65*, 1213-1222.
33. 33. Zhang, Y. L.; Zhang, X.; Fei, X. C.; Wang, S. L.; Gao, H. W. *J. Hazard. Mater.* **2010**, *182*, 877-885.
34. 34. Zhang, G. W.; Wang, A. P.; Jiang, T.; Guo, J. B. *J. Mol. Struct.* **2008**, *891*, 93-97.
35. 35. Ertas, N.; Kara, H. E. S. *Biosens. Bioelectron.* **2015**, *70*, 345-350.